Hans J. Welkoborsky
Peter Jecker
Editors

Ultrasonography of the Head and Neck

An Imaging Atlas

Springer

EXTRAS ONLINE

Ultrasonography of the Head and Neck

Hans J. Welkoborsky • Peter Jecker
Editors

Ultrasonography of the Head and Neck

An Imaging Atlas

Springer

Editors
Hans J. Welkoborsky, MD, DDS, PhD
Department of Otorhinolaryngology
Head and Neck Surgery
KRH Nordstadt Clinic-Academic Hospital
Hannover
Germany

Peter Jecker, MD, PhD
Department of Otorhinolaryngology and Plastic
Head and Neck Surgery
Klinikum Bad Salzungen GmbH
Bad Salzungen
Germany

ISBN 978-3-030-12640-7 ISBN 978-3-030-12641-4 (eBook)
https://doi.org/10.1007/978-3-030-12641-4

This Springer imprint is published by the registered company Springer Nature Switzerland AG
The registered company address is: Gewerbestrasse 11, 6330 Cham, Switzerland

Preface

Ultrasound is a dynamic and interactive process between physician and patient. In the last decades, ultrasound has experienced an enormous expansion in clinical application and indication in the head and neck.

Although established in clinical medicine for many decades, ultrasound is an emerging technique. In recent years, it has been developed into the basic diagnostic imaging technique for examination of the entire neck, salivary glands, thyroid and parathyroid glands, and neck vessels. Other applications comprise the examination of the paranasal sinuses and orbit. Its advantages include the lack of radiation exposure, which makes it suitable, for example, for children or pregnant women, the high resolution of modern ultrasound transducers, and the possibility for a surgeon to correlate ultrasound findings to the intraoperative situation.

Ultrasound is now regarded as the technique that provides the highest sensitivity and diagnostic accuracy for detection of lymph node metastases and salivary gland tumors. New techniques, such as contrast-enhanced ultrasonography, elastography, and 3-D ultrasound, have enhanced the diagnostic accuracy and also the indications for sonographic examinations in the head and neck.

This *Atlas* is dedicated to the office-based use of head and neck ultrasound to provide the best care for patients with head and neck diseases. It covers the physical principles and fundamentals of ultrasonography. The ultrasound characteristics of particular diseases are described in detail in many chapters. Other chapters focus on endosonography, contrast-enhanced ultrasonography, ultrasound in pediatric patients, sonography of large neck vessels, transcranial Doppler sonography, and interventional techniques. Beside many figures with ultrasound characteristics, additional video clips showing typical findings are presented online to demonstrate the dynamic procedure of ultrasound examinations.

Many specialists in head and neck ultrasound have contributed chapters to this book, resulting in a textbook and atlas covering all aspects of head and neck ultrasound. We would like to give special thanks to all the contributing authors for their hard work to make this book successful. We would like to appreciate the fruitful discussions and scientific exchanges that we have experienced with the authors over the years. With some of them, we continue to teach ultrasound courses in Europe and in the United States.

Last but not least, we would like to thank our wives and families for their patience as we worked on this book, as well as Lee Klein, Samantha Lonuzzi and Keerthana Gnanasekeran from Springer for their valuable support and advice. Without the help of all of these amazing people, this book would not have been possible. Thank you all.

Hannover, Germany — Hans J. Welkoborsky
Bad Salzungen, Germany — Peter Jecker

Contents

Contributors

Christoph Arens, MD, PhD Department of Otorhinolaryngology, Head and Neck Surgery, University Hospital Magdeburg, Otto-von-Guericke University, Magdeburg, Germany

Nikolaos Davaris, MD Department of Otorhinolaryngology, Head and Neck Surgery, University Hospital Magdeburg, Otto-von-Guericke University, Magdeburg, Germany

Gabriele H. A. Engelcke, MD Department of Pediatric Radiology, Kinder- und Jugendkrankenhaus Auf der Bult, Hannover, Germany

Urban W. Geisthoff, MD, PhD Department of Otorhinolaryngology, Marburg University Hospital, Marburg, Germany

Michael L. Hinni, MD Department of Otolaryngology–Head and Neck Surgery, Mayo Clinic, Phoenix, AZ, USA

Peter Jecker, MD, PhD Department of Otorhinolaryngology and Plastic Head and Neck Surgery, Klinikum Bad Salzungen GmbH, Bad Salzungen, Germany

Andreas Knopf, MD, PhD Department of Otorhinolaryngology–Head and Neck Surgery, University of Freiburg, Freiburg, Germany

Julian Küstermeyer, MD Department of Otorhinolaryngology, Head and Neck Surgery, KRH Nordstadt Clinic–Academic Hospital, Hannover, Germany

Wolf J. Mann, MD, PhD Department of Otolaryngology, Roemerwall Hospital, Mainz, Germany

Jens E. Meyer, MD, PhD Department of ENT, Head, Neck, and Plastic Surgery, Semmelweis University, Hamburg, Germany

Julia E. Noel, MD Department of Otolaryngology–Head and Neck Surgery, Stanford University School of Medicine, Stanford, CA, USA

Tomislav Novosel, MD Department of Otorhinolaryngology and Plastic Head and Neck Surgery, Klinikum Bad Salzungen GmbH, Bad Salzungen, Germany

Lisa A. Orloff, MD, FACS Department of Otolaryngology–Head and Neck Surgery, Stanford University School of Medicine, Stanford, CA, USA

Ryan K. Orosco, MD Department of Surgery, Division of Otolaryngology–Head and Neck Surgery, University of California San Diego, Moores Cancer Center, La Jolla, CA, USA

Courtney M. Tomblinson, MD Department of Radiology and Radiological Sciences, Vanderbilt University Medical Center, Nashville, TN, USA

Jürgen Weidemann, MD Department of Pediatric Radiology, Kinder- und Jugendkrankenhaus Auf der Bult, Hannover, Germany

Hans J. Welkoborsky, MD, DDS, PhD Department of Otorhinolaryngology, Head and Neck Surgery, KRH Nordstadt Clinic–Academic Hospital, Hannover, Germany

1 History of Head and Neck Ultrasonography

Wolf J. Mann

From neurology to obstetrics/gynecology to internal medicine and finally to all medical and surgical subspecialties, diagnostic ultrasound has its roots in the United States and Europe. Now, each medical discipline worldwide is taking advantage of the wealth of information provided by this technology. Ultrasound has found its place in the scope of modern imaging technology. Since the 60 th of last century, this is true also for the ENT specialty.

1.1 Earliest History

The history of ultrasound started with the discovery of the piezoelectric effect in certain crystals by Pierre Curie and his brother Jacques Curie in Paris in 1880 [1]. A milestone in the development of ultrasound was the tragedy of the *Titanic* in 1912, the same year when Alexander Behm, a physicist from Vienna, invented maritime sonar [2]. In the succeeding decades, the first medical application of ultrasound for therapy was designed, using high-intensity ultrasound to perform craniotomies or destruction of parts of the brain (mainly in the United States) and also to treat patients with rheumatic arthritis or Meniere's disease [3]. At about the same time, Gohr and Wedekind at the University of Köln in 1940 presented the possibility of ultrasonic diagnosis based on echo-reflection methods similar to the one used to detect flaws in metal. However, it was Karl T. Dussik [4], a neurologist and psychiatrist at the University of Vienna, Austria, who applied ultrasound to locate brain tumors and ventricular shift by transmission of ultrasound to the scalp. He presented his initial paper in 1942 and reported further results of the procedure, called "hyperphonography," in 1947. The registrations, called "ventriculograms," were the earliest attempt at the concept of scanning human organs.

W. J. Mann (✉)
Department of Otolaryngology, Roemerwall Hospital, Mainz, Germany
e-mail: Wolf.mann@roemerwallklinik.de

In the mid-1940s, Wolf-Dieter Keidel [5], a German physicist at the Physikalisch-Medizinischen Laboratorium at the University of Erlangen, studied the possibility of using ultrasound as a medical diagnostic tool, mainly for cardiac and thoracic measurements. He discussed his ideas with the engineers of Siemens and at that time also reported the use of ultrasound for diagnosis of paranasal sinus disease.

1.2 The 1950s and 1960s

Between 1950 and 1968, it was mostly echoencephalography that established the role of ultrasound in neurologic diagnosis for endocranial space-occupying lesions [6–8]. However, simultaneous developments took place in gynecology, perinatology [9–11], ophthalmology, cardiology, and other medical disciplines, at that time allowing for the differentiation between cysts and solid tumors [12]. In 1963, Holmes and Howry [13] used ultrasonic scanners through water to examine the head and neck area, in addition to examining the abdomen and the kidney. This diagnostic tool was extended also for examination of neck tumors, for assessment of motion of the lateral pharyngeal wall, and for examination of the thyroid [14–17].

Kitamura et al. [18] used ultrasound for recording of vocal fold motions, and Abramson et al. [19] used ultrasound for the diagnosis of middle-ear effusions. In the 1960s, Kitamura and Kanecko [20] and Gilbricht and Heidelbach [21] reported the use of amplitude-scan (A-scan) ultrasonography for diagnosis of paranasal sinus diseases.

1.3 The 1970s

Between 1970 and 1973, while acting as a surgical intern / resident at the Medical College of Ohio, Toledo (MCO), I met and was inspired by George Döring-Ludwig, an American professor and the founding chairman of the MCO Department of Medicine, who had developed the first appli-

H. J. Welkoborsky, P. Jecker (eds.), *Ultrasonography of the Head and Neck*, https://doi.org/10.1007/978-3-030-12641-4_1

cation of ultrasound to the human body for diagnostic medical purposes at the Naval Medical Research Institute in Maryland in the late 1940s [3]. His research at the Naval Institute focused on detecting gallstones and was classified by the Department of Defense until October 1949. At MCO, I also had the privilege of rotating through the Department of Radiology, which at that time was chaired by Atis K. Freimanis, who had graduated from the medical school of the University of Hamburg, Germany, in 1951. Freimanis was one of the pioneers of B-mode (brightness-mode) ultrasonography at the time of the ultrasonic boom in the 1960s, and he was a gifted teacher. He was well known for his work on the abdomen, the retroperitoneum, the pancreas, aortic aneurysms, and lymph node enlargements. He published seminal papers on sonographic detection of abdominal lymph node enlargement in 1969 and sonography in pancreatic diseases in 1970 [3]. During our discussions, he supported my interest in ultrasound examination of the head and neck, but he was skeptical about whether ultrasound could be used to diagnose sinus diseases.

When I returned to the medical school in Freiburg, Germany, in 1973, I met an engineer, Hermann Kapp, who was working in the Department of Neurology. He generously provided me with a Krautkrämer echoencephalograph, allowing my first attempts to diagnose paranasal sinus disease in Freiburg.

In 1971 the ultrasonic research section at the National Acoustic Laboratory in Sydney, Australia, headed by George Kossoff and William Garrett, reported the use of gray-scale obstetric scans [2]. As early as 1974, initiated by the Department of Neurology at Freiburg Medical School, which at that time had already focused interest on cerebral blood flow using ultrasound, contact was made with Carl Kretz, Chief of Ultrasound Technology in Zipf, Austria, who provided an echograph Type 4100 and, later, a compound B-mode scanner, so that in 1974, using the Combisone (KretzTechnik Zipf, Austria), the first gray-scale imaging of the maxillary and frontal sinus took place.

1975 was the year of my first publication regarding examination of the paranasal sinuses with ultrasound A-scan (Fig. 1.1) [22], and the next year I wrote about examining the

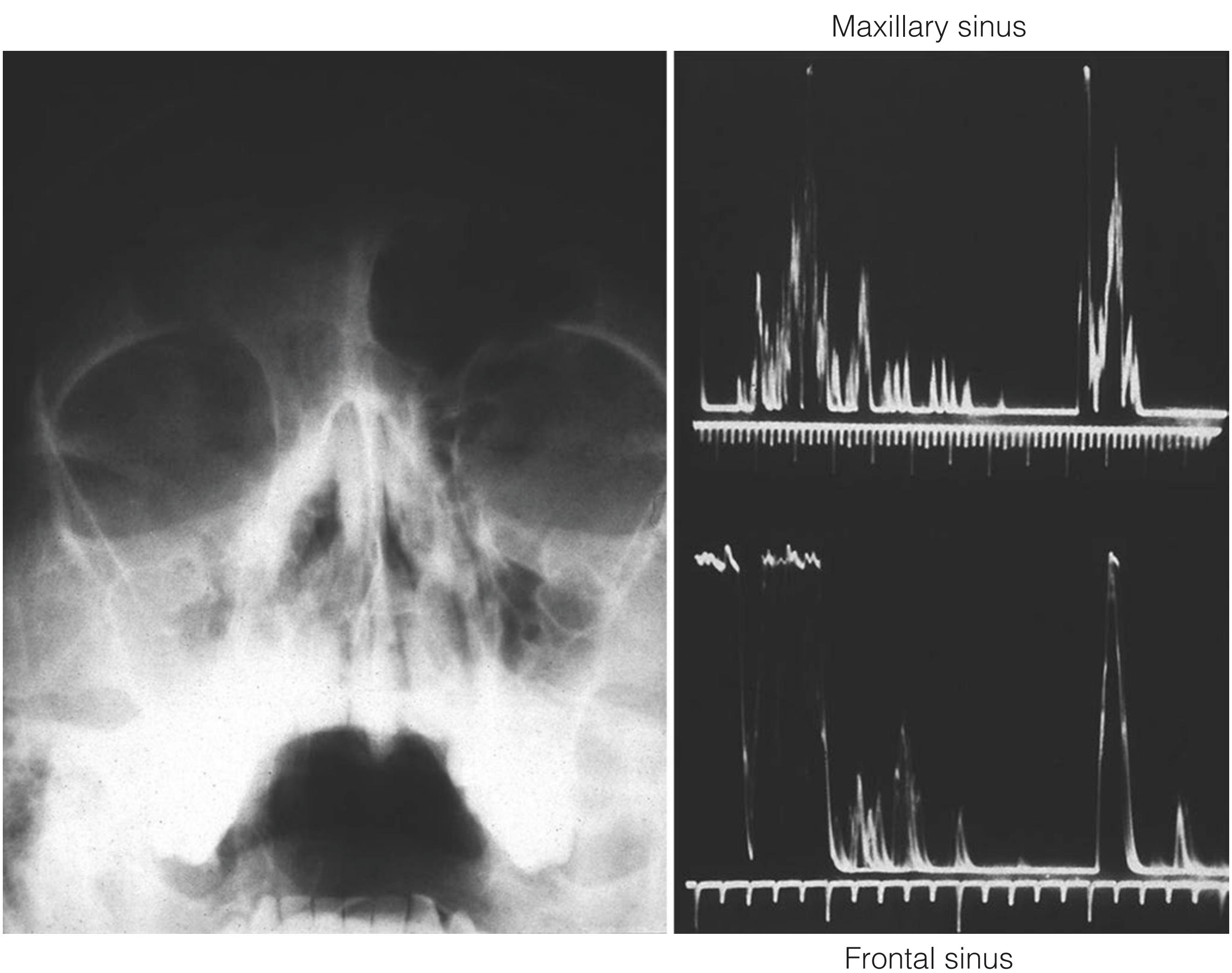

Fig. 1.1 The first gray-scale A scan imaging of the maxillary and frontal sinus

paranasal sinus with compound scanning in a two-dimensional plane [23]. That time, the first real-time ultrasonic scanner (Vidoson, Siemens, Germany) allowed for the generation of 16 black-and-white images per second, although it was too bulky for application in sinus examinations. In the mid-1970s, Wiley et al. [24], Gooding et al. [25], and Scheible and Leopold [26] used B-mode ultrasound technology for clinical evaluation of neck masses. And in the late 1970s and early 1980s, ultrasound was increasingly described in the English, German, and French literature for examination of head and neck lesions, including lesions of the salivary glands [27–29]. Revonta [30] in 1980 introduced A-scan ultrasonography for sinus examination in Finland, and a little later, this technology was also used at Lund University in Sweden by Jannert et al. [31].

1.4 The 1980s and 1990s

In the following years, tissue differentiation technology using gray-scale imaging was combined with A-scan sonography to display tissue differentiation and anatomic orientation in one image. Many new machines designed in the 1980s were based on linear, compound, or sector scanning, using increasing numbers of detectors, higher resolution, and increased storage capacity. Only after the introduction of so-called small parts transducers was the cumbersome examination of the head using abdominal transducers replaced step-by-step. These modern small parts transducers, with variable frequencies, had a dimension of 4 cm or less, improving contact with the surface of the head and neck region (Fig. 1.2). It is understandable that head and neck examination was first validated for parenchymatous organs like the parotid gland or thyroid gland, because their homogenous echostructure allowed for detection of tumors within these organs.

1.5 Expanded Applications

In the mid-1990s, color-coded Doppler sonography was applied to the examination of head and neck lymph nodes, with the aim of differentiating benign from malignant lymphadenopathy by analysis of the vascular perfusion pattern [32]. Transcranial sonography was introduced by otolaryngologists, neurosurgeons, and neurologists to evaluate blood

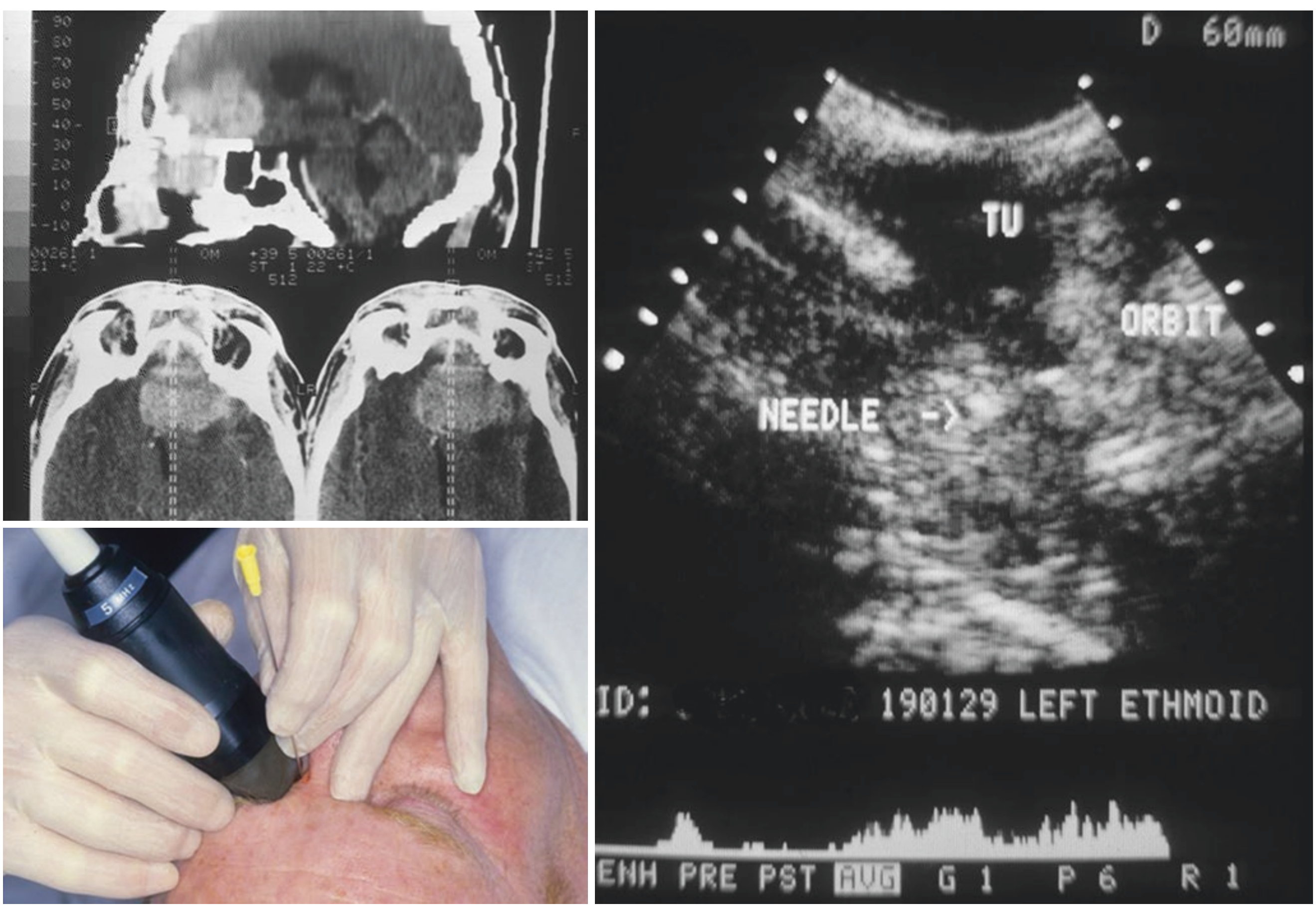

Fig. 1.2 Use of a small parts transducer for guided puncture of a frontal tumor in sonography of the head

flow within the common carotid artery during neck surgery [33, 34], and ultrasound-guided needle aspiration for cytologic examination of diseases of the thyroid, the parotid gland, and the neck became standard [35]. With the introduction of color-coded duplex sonography, it became possible not only to demonstrate vascularity of head and neck tumors and lymph nodes but also to quantify the vascularity and pattern of vascularization. "High-end" ultrasound systems with improved small parts transducers and various frequencies were used for head and neck examinations and were even applied intraoperatively [36, 37]. The introduction of so-called panoramic imaging (which allows for serial images of an entire anatomic area to be composed into ultrasonic tomographic pictures), harmonic imaging [38], 3D imaging, and elastography and the introduction of so-called signal enhancers combined with color-coded-duplex sonography [39] provided additional information on the vascularity of certain neck masses. For example, paragangliomas could be diagnosed in the head and neck without angiography. Parallel to this technical development and the shift from analog to digital technology, this imaging modality became commonplace for almost all medical subspecialties.

National ultrasound societies had been founded in the United States, Germany, Japan, the United Kingdom, Switzerland, and Austria in the 1970s, but specialists focusing on head and neck diseases were nonexistent, except for those performing an initial examination of the neck and thyroid by means of water-bath examination. Umbrella organizations like the American Institute of Ultrasound in Medicine (AIUM), the European Federation for Ultrasound in Medicine (EFSUM), and the World Federation of Ultrasound in Medicine and Biology (WFUMB) evolved. In 1964, the AIUM had broadened its interests away from therapeutic ultrasound applications, focusing on only diagnostic applications.

This focus has grown and diversified ever since. Among regular trinational meetings of the national ultrasound societies of Austria (ÖGUM), Germany (DEGUM), and Switzerland (SGUM), only one presentation in 1979 focused on examination of the head and neck, but a meeting in 2001 included 30 oral presentations on various topics related to head and neck ultrasound examinations. The first textbook summarizing the possible clinical applications of ultrasound to a spectrum of diseases of the head and neck was published in 1984 [40]. Additional textbooks on the topic were published in German in the 1990s [41, 42]. The English literature featured books by Lisa A. Orloff in 2007 [43] and Robert Sofferman and Anil Akuja in 2012 [44]. It was because of individuals like Bruneton in Nice, France, Gritzmann in Austria, van den Brekel in the Netherlands, and Akuja at the Prince of Wales Hospital in Hong Kong that ultrasound has become an integral part of head and neck examination, with a broad spectrum of indications. In the mid-1990s, ultrasound examination of the head and neck became part of the training requirement for a board certification in otolaryngology in Germany, so it became mandatory for each training program to acquire appropriate expertise. At that time, ultrasound schools had developed internationally in Aachen (Westhofen, Jecker), Freiburg (Mann), Erlangen (Iro), Hamburg (Hell), Mainz (Mann, Maurer, Jecker, Welkoborsky, Orloff), Hong Kong (Akuja, Soffermann, Orloff), Amsterdam (van den Brekel), and elsewhere. These programs at first were not found in the United States, but the regular presentation of courses at academy meetings led to the elimination of long-standing obstacles to the incorporation of ultrasound into clinical otolaryngologic practice. In 1998, the American College of Surgeons supported the use of ultrasound by appropriately trained surgeons, and the American Medical Association confirmed ultrasound imaging as being within the scope of practice for appropriately trained physicians.

References

1. Jecker P, Frentzel-Beyme B. The history of head and neck sonography. Laryngorhinootologie. 2002;81:900–5. German.
2. Frentzel-Beyme B. Sonography of head and neck. Praxis (Bern 1994). 2004;93:701–6. German.
3. Woo J. A short history of the development of ultrasound in obstetrics and gynecology. 2002. http://www.ob-ultrasound.net/history1.html. Accessed 15 Feb 2018.
4. Dussik K. Über die Möglichkeit hochfrequente mechanische Schwingungen als diagnostisches Hilfsmittel zu verwerten. Z ges Neurol Psychiat. 1942;174:153–6.
5. Keidel W. Über die Verwendung des Ultraschalls in der klinischen Diagnostik. Ärztl Forsch Z Forschungsergebn Med. 1947;1:349–55.
6. French LA, Wild J, Neal D. Detection of cerebral tumors by ultrasonic pulses: pilot studies on post mortem material. Cancer. 1950;3:705–9.
7. Leksell L. Echoencephalography, I. Detection of intracranial complications following head injury. Acta Chir Scand. 1955;110:301–4.
8. Kazner E, Kunze S, Schiefer E. Die Bedeutung der Echoenzephalographie für die Erkennung epiduraler Hämatome. Langenbecks Arch klin Chir. 1965;310:267–70.
9. Willocks J, Donald I, Duggan TC, Day N. Foetal cephalometry by ultrasound. J Obstet Gynaecol Br Commonw. 1964;71:11–20.
10. Kratochwil A. Ultraschalldiagnostik in Geburtshilfe und Gynäkologie. Stuuttgart: Thieme; 1968.
11. Hoffbauer H. Die Bedeutung der Ultraschalldiagnostik in der Frühschwangerschaft. Elektromedica. 1970;3:227–31.
12. Donald J, Brown TG. Demonstration of tissue interfaces within the body by ultrasonic echo sounding. Br J Radiol. 1961;34:539–42.
13. Holmes JH, Howry DH. Ultrasonic diagnosis of abdominal disease. Am J Dig Dis. 1963;8:12–6.
14. Baum G, Greenwood I. The application of ultrasonic locating techniques to ophthalmology. II. Ultrasonic slit lamp in the ultrasonic visualization of soft tissues. AMA Arch Ophthalmol. 1958;60:263–79.
15. Ossoinig K. Zur Ultraschalldiagnostik der Tumoren des Auges. Mbl Augenheilkunde. 1965;146:321–6.
16. Edler J. The diagnostic use of ultrasound in heart diseases. Acta Med Scand Suppl. 1955;308:32–7.

17. Effert S. Diagnostic value of ultrasonic cardiography. Br J Radiol. 1963;36:302–5.
18. Kitamura T, Kaneko T, Asano H, Muira T. Ultrasonic diagnosis in otorhinolaryngology. Eye Ear Nose Throat Mon. 1969;48:329–37.
19. Abramson DH, Abramson AL, Coleman DJ. Ultrasonics in otolaryngology. An aid in the diagnosis of middle ear fluid. Arch Otolaryngol. 1972;96:146–50.
20. Kitamura TA, Kanecko T. Le diagnostic des affections du sinus maxillaire par ultrasons impulsifs. Ann Oto-Laryngol (Paris). 1965;82:711–4.
21. Gilbricht E, Heidelbach JG. Ultraschall in der Medizin und ihre Anwendungsmöglichkeiten im HNO-Bereich. Z Laryngol Rhino Otol. 1968;47:737–46.
22. Mann W. Die Ultraschalldiagnostik der Nasennebenhöhlen und ihre Anwendung in der Freiburger HNO-Klinik. Arch Otorhinolaryngol. 1975;211:154–5.
23. Mann W. Die Ultraschalldiagnostik der NNH-Erkrankungen mit A- und B-Scan. Laryng Rhinol. 1976;55:48–53.
24. Wiley AL, Zagzebski JA, Tolbert DD, Baujavic RA. Ultrasound B-scans for clinical evaluation of neoplastic neck nodes. Arch Otolaryngol. 1975;101:509–13.
25. Gooding GA, Herzog KA, Lang FC. Ultrasonographic assessment of neck masses. J Clin Ultrasound. 1976;5:248–52.
26. Scheible FW, Leopold GR. Diagnostic imaging in head and neck disease: current applications of ultrasound. Head Neck Surg. 1978;1:1–7.
27. Macridis CA, Kouloulas LA, Kotsimbelas B, Yanoulis G. Zur Diagnose von Speicheldrüsentumoren mit Ultraschall. Elektromedica. 1975;4:130–6.
28. Bruneton JN, Fenart D, Vallicioni J, Demard F. Ultrasonic findings of parotid tumours in 40 patients. J Radiol. 1980;61:151–4. French.
29. Chodosh PL, Silbey R, Oen KT. Diagnostic use of ultrasound in diseases of the head and neck. Laryngoscope. 1980;90:814–7.
30. Revonta M. Ultrasound in the diagnosis of maxillary and frontal sinusitis. Acta Otolaryngol Suppl. 1980;370:1–55.
31. Jannert M, Andreasson L, Holmer N-G, Lörinc P. Ultrasonic examination of the paranasal sinuses. Acta Otolaryngol Suppl. 1982;389:1–52.
32. Schreiber J, Mann W, Lieb W. Farbduplexsonographische Messung der Lymphknotenperfusion. Ein Beitrag zur Diagnostik der zervikalen Metastasierung. Laryngo Rhino Otol. 1993;72:187–92.
33. Mann WJ, Beck A, Schreiber J, Maurer J, Amedee RG, Gluckmann JL. Ultrasonography for evaluation of the carotid artery in head and neck cancer. Laryngoscope. 1994;104:885–8.
34. Maurer J, Ungersböck K, Amedee RG, Mann WJ, Perneczky A. Transcranial Doppler ultrasound recording with compression tests in patients with tumors involving the carotid artery. Skull Base Surg. 1993;3:11–5.
35. Knapp I, Mann W, Wachter W. The value of ultrasound-controlled fine-needle biopsy in the diagnosis of possible neck tumors. Laryngorhinootologie. 1989;68:683–9. German.
36. Ecke U, Gosepath J, Mann WJ. Initial experience with intraoperative ultrasound in navigated soft tissue operations of the neck and below the base of the skull. Ultraschall Med. 2006;27:49–54.
37. Stetter S, Jecker P, Mann WJ. Einsatz des intraoperativen Ultraschalls in der Speicheldrüsenchirurgie. Ultraschall Med. 2006;27:159–63.
38. Jecker P, Maurer J, Mann WJ. Improved tumor site and contrast resolution in ultrasound diagnosis by using harmonic frequencies. Laryngorhinootologie. 2001;80:203–8. German.
39. Jecker P, Engelke JC, Westhofen M. Possible application of a signal enhancer for duplex ultrasound in otorhinolaryngology. Laryngorhinootologie. 1998;77:289–93. German.
40. Mann W. Ultraschall im Kopf/Hals-Bereich. Berlin/Heidelberg: Springer; 1984.
41. Hell B. Atlas der Ultraschalldiagnostik im Kopf-Hals-Bereich. New York: Georg-Thieme-Verlag; 1990.
42. Mann W, Welkoborsky HJ, Maurer J. Kompendium Ultraschall im Kopf-Hals-Bereich. New York: Thieme-Stuttgart; 1997.
43. Orloff LA. Head and neck ultrasonography. San Diego: Plural Publishing; 2007.
44. Soffermann RA, Akuja AT. Ultrasound of the thyroid and parathyroid glands. Heidelberg/New York: Springer; 2012.

2 Physics and Principles of Ultrasound

Ryan K. Orosco and Lisa A. Orloff

2.1 Introduction

This book contains a wealth of information about head and neck ultrasound. In order to take full advantage of this content, one must possess a strong understanding of the physics of ultrasound and the fundamentals of ultrasound imaging. Knowledge of the principles of ultrasound physics is not an absolute requisite for utilizing ultrasound, but it will make possible a higher level of technical mastery and will allow for high-quality implementation of ultrasound into clinical practice.

A clinical ultrasound image is the end result of complex interaction between hardware design elements and software processing. The goal of this chapter is to ensure that clinicians using this technology are aware of the key concepts and principles of ultrasound physics, without having to possess advanced understanding of the underlying engineering. This chapter addresses the basics of wave properties, ultrasound wave generation and reception, and the behavior of sound in tissue. Common ultrasound artifacts are explained from the physics perspective, and the special case of Doppler is discussed.

R. K. Orosco
Department of Surgery, Division of Otolaryngology–Head and Neck Surgery, University of California San Diego, Moores Cancer Center, La Jolla, CA, USA

L. A. Orloff (✉)
Department of Otolaryngology–Head and Neck Surgery, Stanford University School of Medicine, Stanford, CA, USA
e-mail: lorloff@stanford.edu

2.2 Sound and Ultrasound Waves

Sound waves are longitudinal waves, which cause particles and energy to move (propagate) through a medium (gas, liquid, solid). This is in contrast to transverse waves, which are like the ripples caused by dropping a stone in a bucket of water. In the water ripple example, the wave energy moves across the surface of the water, but the water particles themselves do not propagate—they just move vertically up and down.

Sound wave propagation is a familiar concept that we encounter frequently in daily life. Sound travels through the air, water, and ground. Sound energy causes compression and rarefaction of the molecules in the material through which it travels. These compressions and rarefactions are displayed graphically and mathematically as a sinusoidal wave. Ultrasound waves and audible sound waves behave in a similar fashion. They travel (propagate), reflect (echo), and are absorbed to varying degrees depending on the material with which they interact. For clinical ultrasound, the sound within the echo wave that is received by the ultrasound transducer is translated into an image, with brightness (B-mode) proportional to the amplitude of reflection.

The mathematical characteristics of a sine wave are amplitude, frequency, and wavelength. Amplitude is the height of a wave, which can be thought of as a corollary of sound intensity. Wave velocity can be calculated as the product of the frequency (f) and wavelength (λ): wave velocity = $f\lambda$. The higher the sound frequency, the shorter the wavelength. The frequency is reported in hertz (Hz), which represents the number of wave cycles per second: f = cycles/second. A 1 Hz wave has one cycle per second. A 1 MHz (1,000,000 Hz) wave has one million cycles per second. The normal hearing spectrum (20 Hz–20 kHz) includes frequencies well below those used in ultrasonic applications (Fig. 2.1). In general, 7.5–15 MHz is the ideal ultrasound frequency range for neck imaging.

H. J. Welkoborsky, P. Jecker (eds.), *Ultrasonography of the Head and Neck*, https://doi.org/10.1007/978-3-030-12641-4_2

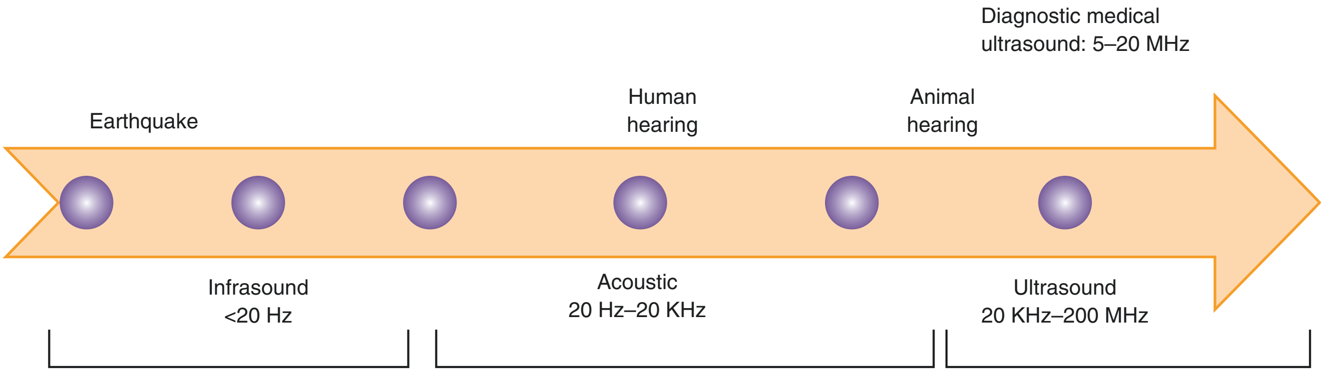

Fig. 2.1 Sound frequency spectrum

2.3 Ultrasound Wave Generation and Reception

Ultrasound waves are generated by an array of microscopic piezoelectric crystals. When subjected to electrical energy, the crystals change shape and generate ultrasound waves that are passed into tissues for clinical ultrasound imaging. Reflecting back, the ultrasound echo vibrates and distorts the crystal shape, translating an electrical signal back to a computer. The same crystal can be used to generate and receive ultrasound signals. Any given crystal—or the group of crystals called a "sector"—spends most of its time receiving sound information. The ultrasound machine has complex algorithms that alternate between generating and receiving modes in order to optimize image quality. It should be noted that piezoelectric crystals can be damaged by heat and mechanical forces, so care should be taken when handling the ultrasound transducer, and it should not be heat sterilized.

The piezoelectric crystals in clinical ultrasound devices are made of inorganic synthetic materials, commonly lead zirconate titanate (PZT). The ultrasound transducer consists of the electrical interface, material used for insulation and acoustic matching, and an array of crystals. For head and neck applications, the crystal array is linear, but other geometries exist. Depending on the ultrasound transducer, there may be multiple rows of crystals. The linear configuration affords planar ultrasound imaging, which is analogous to the familiar planar imaging of CT and MRI.

2.4 Ultrasound in Tissues

Sound speed, or velocity, depends on the material through which the wave is traveling. This velocity is positively correlated with the material's density—the denser the material, the faster the sound waves travel. In air, the velocity of sound is about 330 m/s. Knowing the wave velocity in a given medium and the time from sound generation to reception allows calculation of the distance that a wave has traveled from the source to the receiver. This is why one can estimate how far away one is from a lightning strike by counting the seconds between seeing the flash (source) and hearing the thunder crack (receiver). To bring this into medical context, consider the sound velocity in various body tissues: 1459 m/s in adipose tissue, 1480 m/s in water, and 1580 m/s in muscle. The velocity of sound in dense bone tissue is even faster: >4000 m/s. Ultrasound machines take into account the wave parameters of frequency, amplitude, and velocity as they generate the clinical images. Several more key concepts related to wave propagation in tissues will be addressed in the next sections: impedance, reflection, transmission, attenuation, and spatial resolution.

2.4.1 Acoustic Impedance, Reflection, and Transmission

Acoustic impedance is the product of material density and the acoustic velocity: Impedance = density × acoustic velocity. Because different materials have different densities, they also have different impedances. When a sound wave reaches the interface between two dissimilar materials, some of the energy is *transmitted* into that new medium, and some is *reflected* back. The magnitude and direction of the reflected and transmitted energy depend on the angle of the initial wave signal (the incident angle) and the difference in impedance properties of the two materials. Similar to the scenario of a laser beam fired at a mirror, the reflected energy returns at the same angle (compared with a normal, or perpendicular, reference), but in the negative direction of the incident beam. The portion of the wave that is not reflected will pass into the second material, but it does so at a slightly different angle. This new angle occurs because of the property of *refraction*, explained by Snell's law. For now, just focus on wave transmission and reflection in the purest situation—when the sound wave hits the boundary interface at a 90-degree angle (perpendicular to the interface). In this situation, the speed and wavelength of this reflected wave are the same as that of the incident wave.

The greater the difference, or mismatch, in material *impedance*, the more wave energy is reflected. Imagine a ball passing through a material with low impedance (air) that strikes an interface with high impedance (a brick wall)—most of the energy is reflected back. This imperfect example should suffice to convey the concept of reflection: If there is a small mismatch in impedance between the two mediums at the interface, most of the sound energy is transmitted through, with little reflected.

Understanding the concepts of impedance, reflection, and transmission provides a physics-based explanation of what we intuitively understand when we are unable to see beyond the interface of two very dissimilar tissues, such as the soft tissues of the neck and the air-filled lumen of the trachea or the soft tissues of the parotid and the bony mandible. This also explains why ultrasound gel is needed for "contact coupling." The gel removes two boundary conditions (ultrasound transducer/air and air/skin) that would otherwise cause considerable signal loss and prevent imaging altogether.

2.4.2 Attenuation

Attenuation is another important concept that is likely to be familiar in our daily lives. The concept is that the amplitude of a sound pressure wave degrades, or decreases, as it travels through a medium. This degradation is a result of energy being absorbed by the medium, and some energy loss through scattering effects. When performing ultrasound, it is important to recognize that energy is deposited into the patient's tissues and converted into heat. Practically, routine clinical ultrasonography of the head and neck does not raise the tissue temperatures enough to cause harm. Still, the concept of "ALARA"—as low as reasonably achievable—is advocated in the practice of clinical ultrasonography. Making every reasonable effort to maintain exposures to ultrasound heat as low as practical serves to minimize the risk of potential thermal injury to the patient.

Intuitively, the greater the distance a wave travels through a medium, the greater the attenuation along that path. It is important to note that attenuation is not a linear phenomenon; it follows the inverse square law. The signal intensity (wave amplitude) decreases by the square of the distance: Intensity = 1/distance^2. Attenuation is also proportional to the frequency: Attenuation (measured in decibels [dB]) = ½ × frequency × distance. There is less attenuation with waves that have a longer wavelength (lower frequency). Based on these characteristics, extremely low-frequency waves can pass through the ocean and even the earth's surface to communicate across distances. The clinical correlate of this concept is that the imaging of superficial structures is best accomplished with high-frequency ultrasound transducers, whereas deeper structures require lower-frequency transducers (or alterations in sound frequency generation).

Clinical ultrasound devices automatically compensate for attenuation using "time-gain compensation." The signal from more distant objects is increased (scaled) in order to counteract the signal attenuation. Because higher-frequency signals attenuate faster (in shorter distances from the source), more time-gain compensation is required. *Gain* (or in B-mode, brightness) can also be manually adjusted on most modern clinical ultrasound devices, either as a global (overall) gain or at various image depths. Note that there are limits to the usefulness of gain because it amplifies noise, or undesirable signal information, in addition to the true echo signal of interest.

2.4.3 Spatial Resolution

Spatial resolution is the final key concept to consider when performing clinical ultrasound. In today's digital world, resolution is an intuitive concept, as it is analogous to pixel resolution. When we ask ourselves how clear the ultrasound image is, we are really talking about the ability of the imaging system to differentiate between two objects, or two points. If two points are closer to each other than the spatial resolution of the system, the resultant image will display a single point that is a conglomeration of the two separate points. In clinical ultrasound systems, spatial resolution differs depending on whether the objects are perpendicular to the transducer or parallel with it (lateral or axial resolution).

The lateral resolution depends on the width of the ultrasound beam. Depending on the ultrasound system, the beam can be focused at one or multiple distances to alter the lateral resolution. Resolving two side-by-side points that are in line with or parallel to the transducer (axial resolution) is a function of ultrasound wavelength. The higher the frequency, the finer the axial resolution. But because these higher frequencies also come with more attenuation, there is always a tradeoff. Just as with other imaging parameters, most clinical ultrasound systems allow for the depth of focus and frequency to be adjusted. These adjustments allow one to optimize the resolution in various clinical situations.

2.5 Artifacts in Ultrasound Imaging

Ultrasound imaging artifacts are erroneous representations of the anatomy that result from the physical interaction between sound waves and tissues and the manner in which the resultant sound echo is processed and displayed by the computer. Several assumptions are made by the ultrasound computer: that the echoes received by the transducer originated from the main ultrasound beam from the same transducer; that an echo returns to the transducer after a single reflection; that the depth of an object is directly related to the amount of time for an ultrasound pulse to return to the transducer as an echo; that the speed of sound in human tissue is constant (generally about 1540 m/s); that ultrasound waves (incident beam and reflection) travel in a straight path (without refraction); and that the signal is uniformly attenuated in human tissue [1]. When these generalized assumptions are applied to real-world systems, ultrasound artifacts invariably result.

Without a thorough understanding of ultrasound physics, imaging artifacts can be misinterpreted, misclassified, and misunderstood. Although incorrect interpretation of artifacts can interfere with accurate diagnosis, proper interpretation can actually provide clues and be diagnostic for certain entities.

Two-dimensional ultrasound mode (2D mode), sometimes referred to as brightness (B-mode), is the standard mode used for head and neck ultrasound. In this mode, one will encounter reverberation, comet tail, mirror image, shadowing, and posterior enhancement artifacts. The key concepts presented earlier can be applied to understand these common artifacts. In 2D mode, refraction, beam width, range ambiguity, and speed error artifacts can also occur [2], but these are infrequently applicable in head and neck ultrasonography. Doppler imaging artifacts also exist [2] but are seldom encountered in head and neck ultrasound practice, which focuses more on anatomic architecture and qualitative vascular flow than quantitative Doppler.

2.5.1 Reverberation Artifact

Because the computer assumes that an echo returns to the transducer after a single reflection, reverberation artifact occurs in the presence of parallel highly reflective interfaces that cause repeated reflections (Fig. 2.2). This artifact is encountered when imaging the trachea, because of a marked impedance mismatch. The ultrasound waves encounter the interface between the soft tissue and tracheal cartilage, and a reflected signal echoes back to the transducer. This surface of the cartilage is displayed on the image at its true anatomical depth, but some ultrasound waves pass into the air of the tracheal lumen and encounter another interface (air/soft tissue) at the posterior trachea, again with a high-impedance mismatch. This causes another reflected wave, resulting in another echo back to the transducer. The second echo takes longer to return to the transducer and therefore has a longer apparent distance traveled. The result is an artifact signal that is deeper than the true anterior tracheal location. This same process repeats when the echo, traveling toward the transducer, hits the anterior tracheal wall: Some of the wave is reflected back through the air, and some makes its way back to the transducer. The reverberation artifact is displayed as multiple evenly spaced linear reflections deep to the true object boundary. Because the signal intensity attenuates each time, the size of the artifact reflections diminishes with each reflection. Moving the transducer to view the trachea from different incident angles can help identify and reduce confusion from reverberation artifact.

2.5.2 Comet-Tail Artifact

Comet-tail artifact (Fig. 2.3) is a special type of reverberation artifact that is commonly encountered in the thyroid. Echogenic foci within the thyroid can be microcalcifications, which are highly suggestive of malignancy, but they can also be caused by inspissated or clustered colloid crystals that produce a comet-tail artifact [3]. Although indicative of a

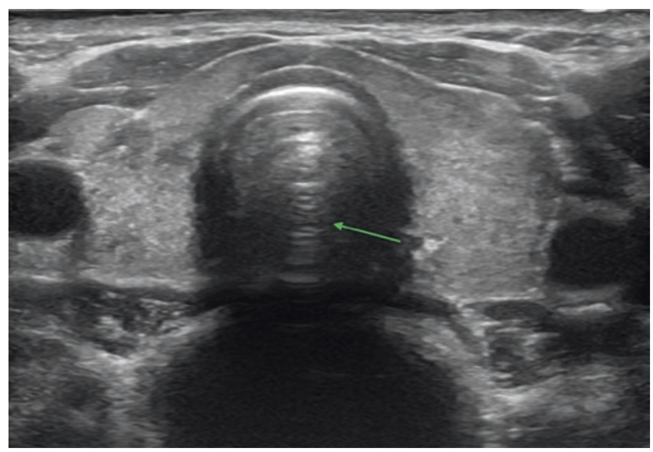

Fig. 2.2 Midline transverse view of the trachea with reverberation artifact (*green arrow*)

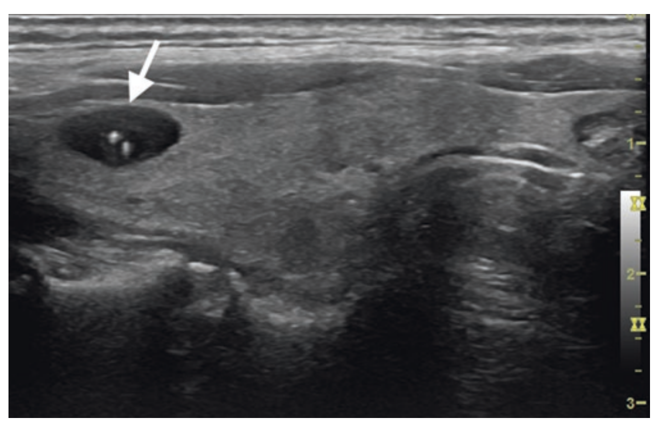

Fig. 2.3 Colloid cyst within the thyroid (*arrow*) with internal comet-tail artifact

benign nodule, it is not absolutely pathognomonic for such [4]. The distance between the two high-impedance mismatch interfaces is so small in these collections that individual reverberations are not visible. Instead of seeing multiple parallel reverberation artifact reflections of decreasing size, as with the trachea example in Fig. 2.2, a smeared "comet-tail" artifact is seen on the image.

2.5.3 Mirror-Image Artifact

The mirror-image artifact occurs when an object of interest is located near and superficial to a surface with high impedance. It is manifested as a "mirror image" or false object that is displayed equidistant from the reflective surface but on the opposite, deep side (Fig. 2.4). It occurs because reverberations between the reflective surface and the object effectively prolong the path time for the beam. Changing the incident angle of the transducer can help distinguish this artifact.

2.5.4 Shadowing Artifact

When ultrasound waves encounter a high-impedance tissue, most of the energy is reflected. As a result, the tissue immediately beyond the high-impedance interface appears obscured or void. This shadowing artifact (Fig. 2.5) is seen with dense structures such as bone, salivary calculi, and coarse calcifications within the thyroid. Knowledge of this artifact can help distinguish calcifications from colloid-related echogenic foci within the thyroid. Microcalcifications may be more difficult to distinguish, however, because they are echogenic or bright, but too small to produce a significant shadow.

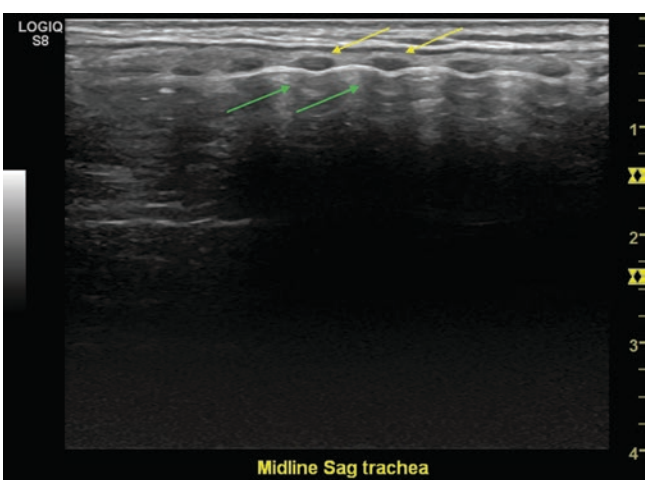

Fig. 2.4 Midline sagittal view of the trachea shows mirror-image artifact (*green arrows*) deep to the cartilaginous rings (*yellow arrows*)

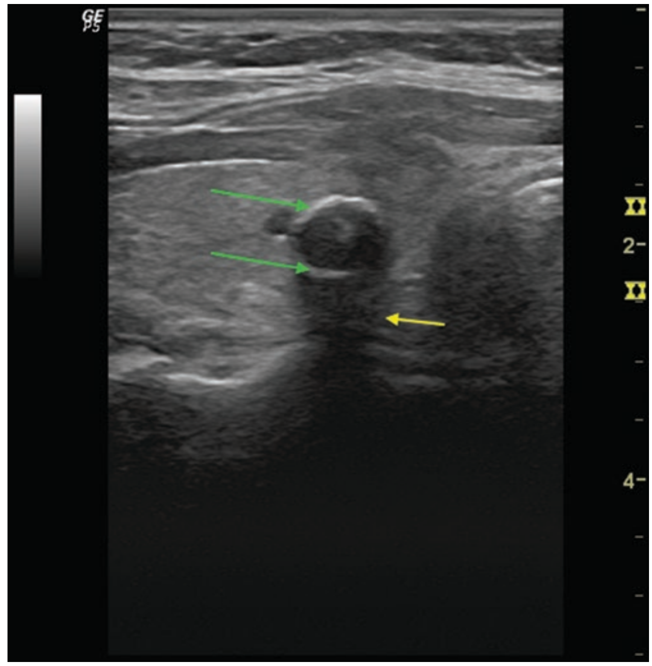

Fig. 2.5 Coarse rim calcification (*green arrows*) of a small thyroid nodule causes shadowing artifact both within the nodule and posterior (deep) to the nodule (*yellow arrow*)

2.5.5 Posterior Enhancement Artifact

Enhancement (Fig. 2.6) appears as a bright area deep to a hypoechoic or anechoic area or a low-impedance object. Compared with the tissue immediately lateral (beside) it, more sound energy passes through the object. Subsequently, there is more sound energy striking the area behind the object. These waves with relatively higher energy are reflected back to the transducer and displayed as a brighter signal behind (posterior) to the object. Posterior enhancement occurs when imaging cysts and some tumors such as pleomorphic adenomas within salivary tissue.

2.6 Doppler

Up to this point, we have been thinking about ultrasound imaging situations where the signal generator/receiver (ultrasound transducer) and the target object (anatomic tissue) are both stationary. The Doppler effect comes into play in situations where either the sound source, sound receiver, or target object are moving. The Doppler effect occurs when reflected sound waves get compressed or rarefied due to relative motion among these elements. This artificial compression or rarefication results in a sound frequency change.

This phenomenon is commonly explained using the real-world example of a siren on an ambulance as it drives down the road and passes an observer. The observer hears the high-pitched siren sound as the ambulance approaches. Because the

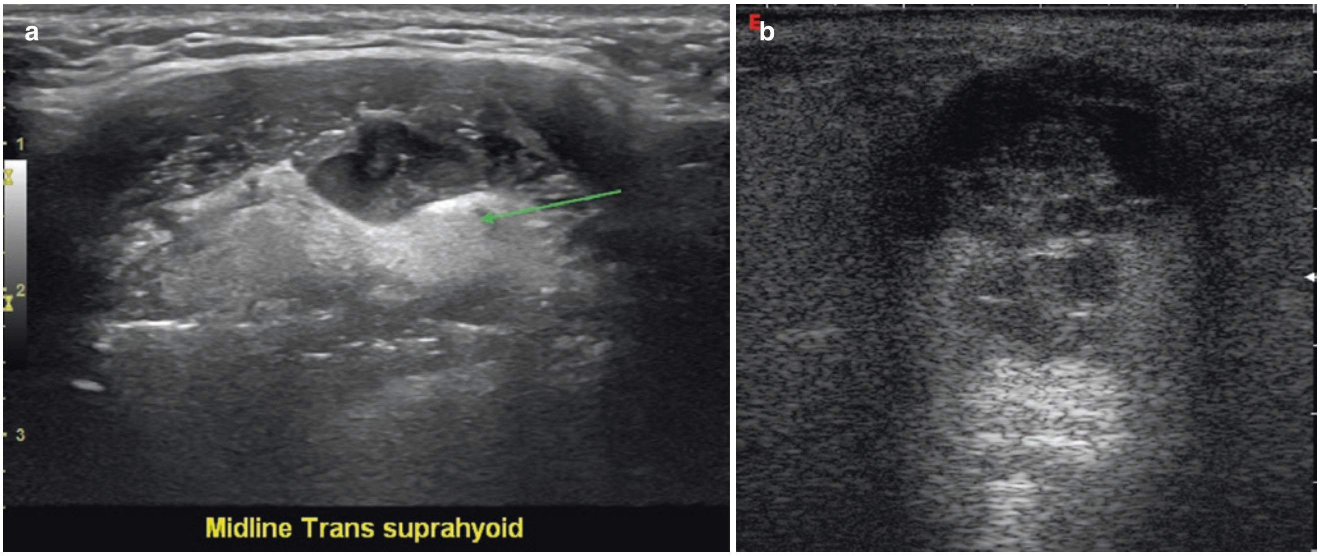

Fig. 2.6 Posterior enhancement artifact. (**a**) Midline transverse view of an incidentally noted thyroglossal duct cyst with posterior enhancement artifact (*green arrow*). (**b**) Pleomorphic adenoma of the parotid gland with posterior enhancement artifact

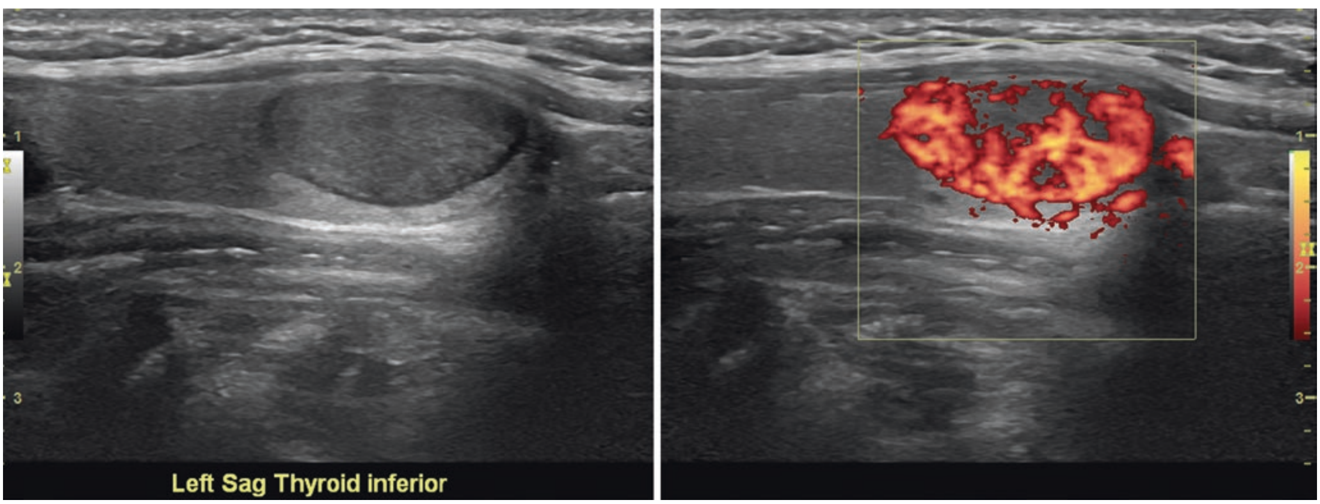

Fig. 2.7 *Left*, B-mode view of a hypoechoic thyroid nodule (follicular neoplasm by cytology). *Right*, Power Doppler view showing intense vascularity

sound waves and the sound source (siren) are moving toward the observer, this pitch (frequency) is artificially higher. For the split second when the vehicle has moved right next to the observer (perpendicular to the observer), the pitch of the siren is just as it would be if the vehicle were stopped. As the ambulance speeds on past the observer, the siren sounds lower-pitched (lower-frequency). In this scenario, the observer is stationary, and the sound source is moving. For clinical ultrasound scenarios, it is the target tissue (or fluid, such as blood) that is moving, with the sound generator/receiver in a fixed position. Phase changes can also be used for motion detection, but we will focus on the concept of frequency change for the purposes of understanding the concept.

The Doppler effect principle is applied to evaluate vascular flow with clinical ultrasound. The two main Doppler modes are *color-flow Doppler* and *power Doppler*. Color-flow Doppler distinguishes the directionality of flow (away or toward the transducer) and displays the different directions with a color scale. The algorithm used to produce color-flow Doppler images is affected by noisy signals (high signal/noise ratio), so it automatically filters out low-flow information in an effort to minimize this shortcoming. Accordingly, small veins and low-flow structures are not visible in color-flow mode. The power Doppler mode overcomes the shortcoming with regard to low-flow signals by mapping an integrated power map of the Doppler signal, effectively increasing the signal/noise ratio. This setting shows flow regardless of directionality and is better for detecting low-flow structures, but the information about flow direction is lost (Fig. 2.7). For most head and neck ultrasound purposes, information about flow direction is less important than the detection of flow itself, so power Doppler is commonly used.

2.7 Summary

The principles discussed in this chapter represent the minimum knowledge of sound wave physics needed to optimize the performance and interpretation of ultrasound studies. Fortunately for the modern-day ultrasonographer, the powerful computer engineering available in even entry-level ultrasound systems enables acquisition of high-resolution anatomic images with little effort. The examiner can focus on image interpretation, with only minor adjustments in equipment settings and accommodations for artifacts. For more in-depth discussion, the reader is referred to the suggested resources below.

References

1. Feldman MK, Katyal S, Blackwood MS. US artifacts. Radiographics. 2009;29:1179–89.
2. Prabhu SJ, Kanal K, Bhargava P, Vaidya S, Dighe MK. Ultrasound artifacts: classification, applied physics with illustrations, and imaging appearances. Ultrasound Q. 2014;30:145–57.
3. Hoang JK, Lee WK, Lee M, Johnson D, Farrell S. US Features of thyroid malignancy: pearls and pitfalls. Radiographics. 2007;27:847–60; discussion 861–5.
4. Wu H, Zhang B, Li J, Liu Q, Zhao T. Echogenic foci with comet-tail artifact in resected thyroid nodules: not an absolute predictor of benign disease. PLoS One. 2018;13:e0191505.

Suggested Reading

Gibbs V, Cole D, Sassano A. Ultrasound physics and technology E-book: how, why and when. Philadelphia: Elsevier Health Sciences; 2011.

Hoskins PR, Martin K, Thrush A. Diagnostic ultrasound: physics and equipment. Cambridge: Cambridge University Press; 2010.

Zagzebski JA. Essentials of ultrasound physics. St. Louis: Mosby; 1996.

Ultrasound Anatomy of the Head and the Neck

3

Peter Jecker

3.1 General Notes

The correct interpretation of ultrasound findings requires an excellent knowledge of the neck anatomy. Thus, an anatomic atlas should always be available in case of unknown findings. Furthermore, the examiner should be familiar with the sonographic appearance of the normal neck structures, which are often used as landmarks to facilitate the reproducibility of ultrasound findings by different examiners. These structures or landmarks include organs (such as the thyroid or salivary glands), bony structures or cartilages, muscles, blood vessels, and nerves. The purpose of this chapter is to present these structures in the healthy neck.

3.2 Settings of the Ultrasound Device and Starting the Examination

Normally we prefer a linear scanner with a frequency between 7.5 and 10 MHz. If postoperative scar formation of the neck tissue is present, the use of a lower frequency is necessary. Additionally, sector imaging is sometimes advantageous, especially if large structures should be described.

The neck examination should always start with an area where the device adjustment can be checked [1]. We prefer starting the examination with a view of the thyroid gland and the surrounding vessels, i.e., the common carotid artery and internal jugular vein (Fig. 3.1). In this section, the carotid artery wall shows a high echogenicity, whereas the lumen of the vessels should be hypoechoic (Video 3.1). The quality of the thyroid's echo is between the echogenicity of both structures. This section through the thyroid gland allows fast and easy adjustment of the device. Then we examine the medial neck compartment, followed by both lateral compartments. After this, the region of the salivary glands is examined, followed by the tongue and the tongue base.

3.3 Systematic Head and Neck Ultrasound Examination: Normal Findings

3.3.1 The Medial Neck Compartment, Thyroid, and Larynx

The thyroid is the main organ in the medial neck compartment (Video 3.2). The thyroid lobes are connected by the isthmus, which can be seen in both transverse and sagittal section (Figs. 3.2 and 3.3). The thyroid of the healthy patient is more or less homogenous, and its echogenicity is similar to the echogenicity of the large salivary glands [1, 2]. The tracheal cartilages can also be seen, producing artificial reverberation echoes (Fig. 3.2). Lateral to the thyroid, the large blood vessels (the common carotid artery and more laterally, the internal jugular vein) can be found (Fig. 3.4). Sometimes, the vagal nerve becomes visible next to the blood vessels (Fig. 3.1). In the depth, the thyroid adjoins the scalene muscles and the vertebral column. Infrahyoid muscles can be seen in front of the thyroid gland. Differentiation of the infrahyoid muscles would be possible without any problem when using a modern ultrasound device.

The upper esophagus (Fig. 3.5) can commonly be seen under the left thyroid lobe, next to the vertebral column [3]. Parts of the esophagus are covered by the acoustic shadow of the trachea. The esophagus is characterized by an onion-like pattern. Especially in the sagittal plane, swallowing of saliva can be observed (Video 3.3). Sometimes, the esophagus also can be seen under the right thyroid lobe (Fig. 3.6); in rare

Electronic Supplementary Material The online version of this chapter (https://doi.org/10.1007/978-3-030-12641-4_3) contains supplementary material, which is available to authorized users.

P. Jecker (✉)
Department of Otorhinolaryngology and Plastic Head and Neck Surgery, Klinikum Bad Salzungen GmbH, Bad Salzungen, Germany
e-mail: peter.jecker@klinikum-badsalzungen.de

H. J. Welkoborsky, P. Jecker (eds.), *Ultrasonography of the Head and Neck*, https://doi.org/10.1007/978-3-030-12641-4_3

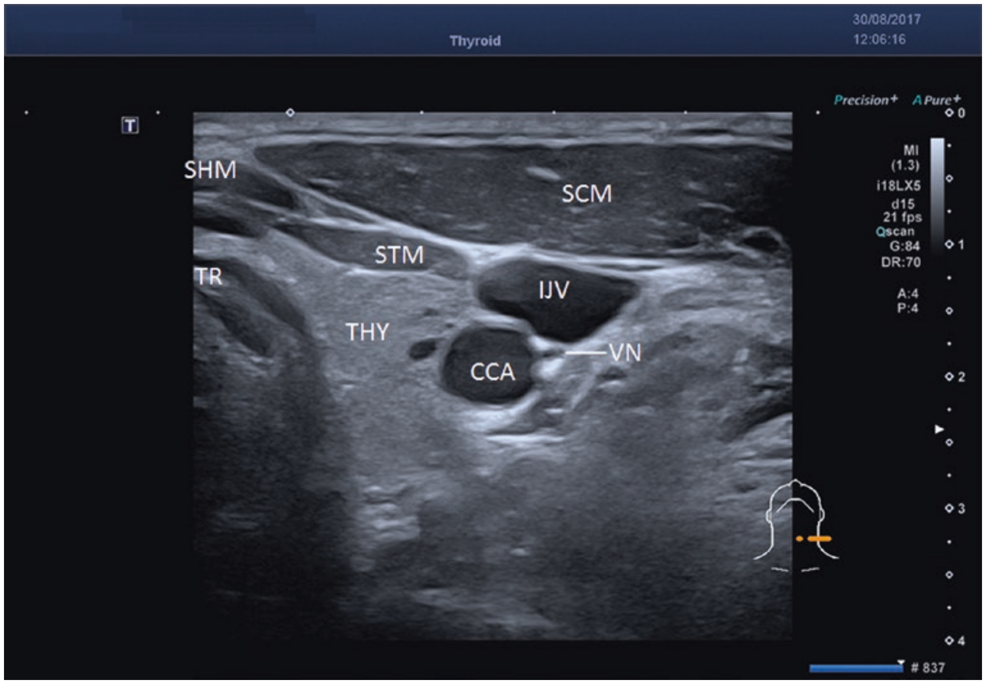

Fig. 3.1 Basic adjustment of the ultrasound device using a standardized plane through the thyroid gland (THY), the common carotid artery (CCA), and the internal jugular vein (IJV). SCM sternocleidomastoid muscle, SHM sternohyoid muscle, STM sternothyroid muscle, TR trachea, VN vagal nerve

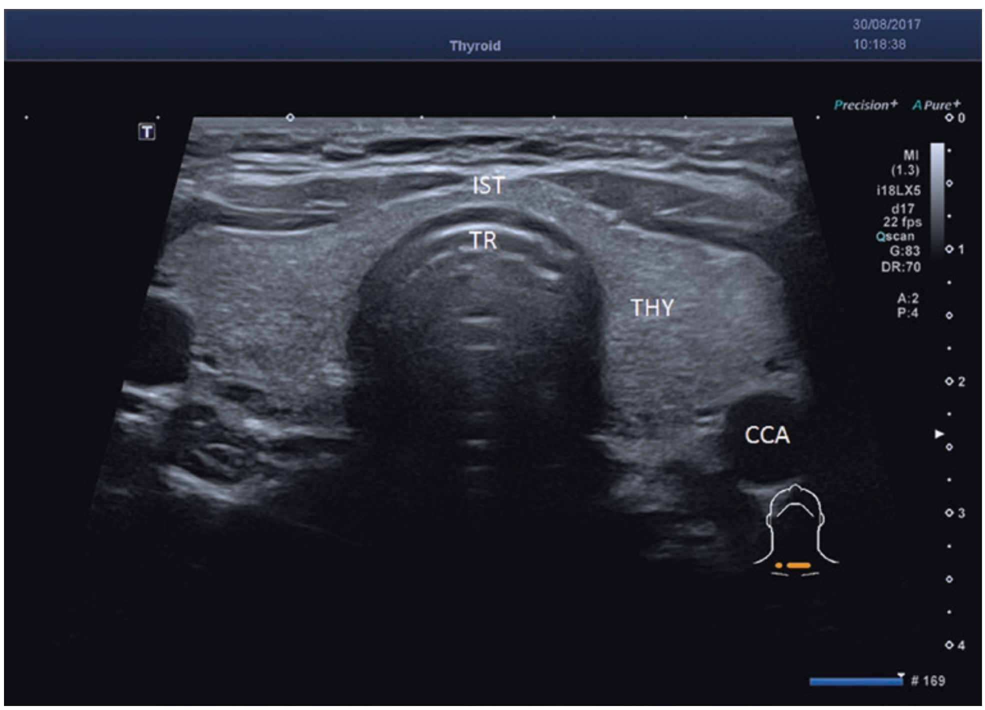

Fig. 3.2 Lower medial cervical compartment with the homogenous thyroid gland (THY), transverse plane. CCA common carotid artery, IST isthmus, TR trachea

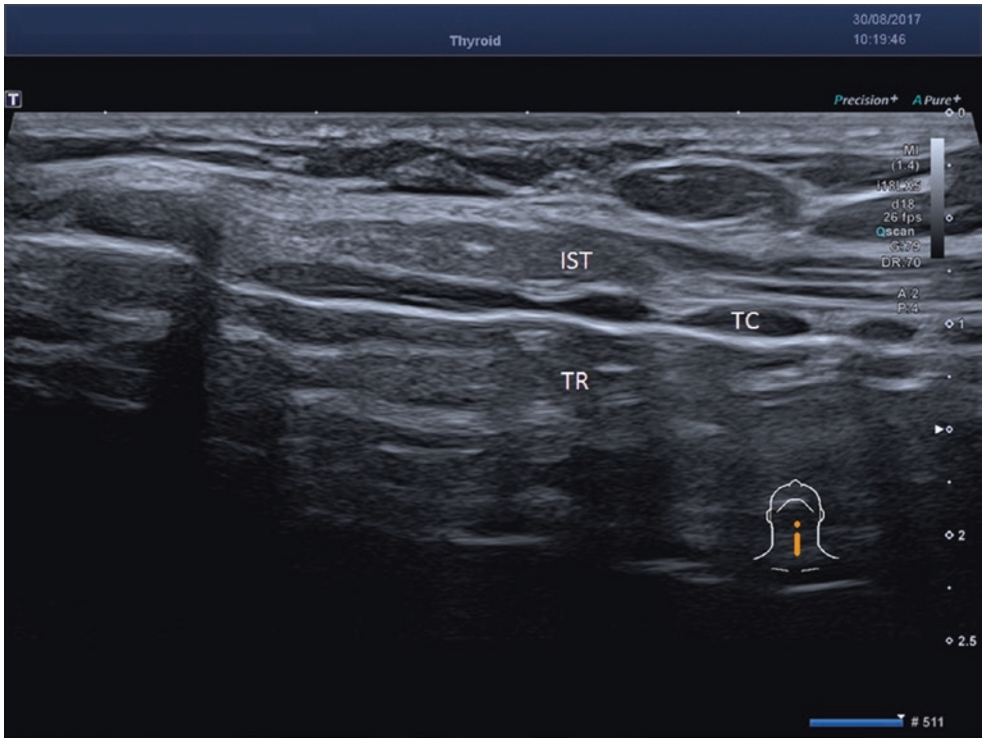

Fig. 3.3 Isthmus of the thyroid (IST), sagittal plane. TC tracheal cartilage, TR tracheal lumen

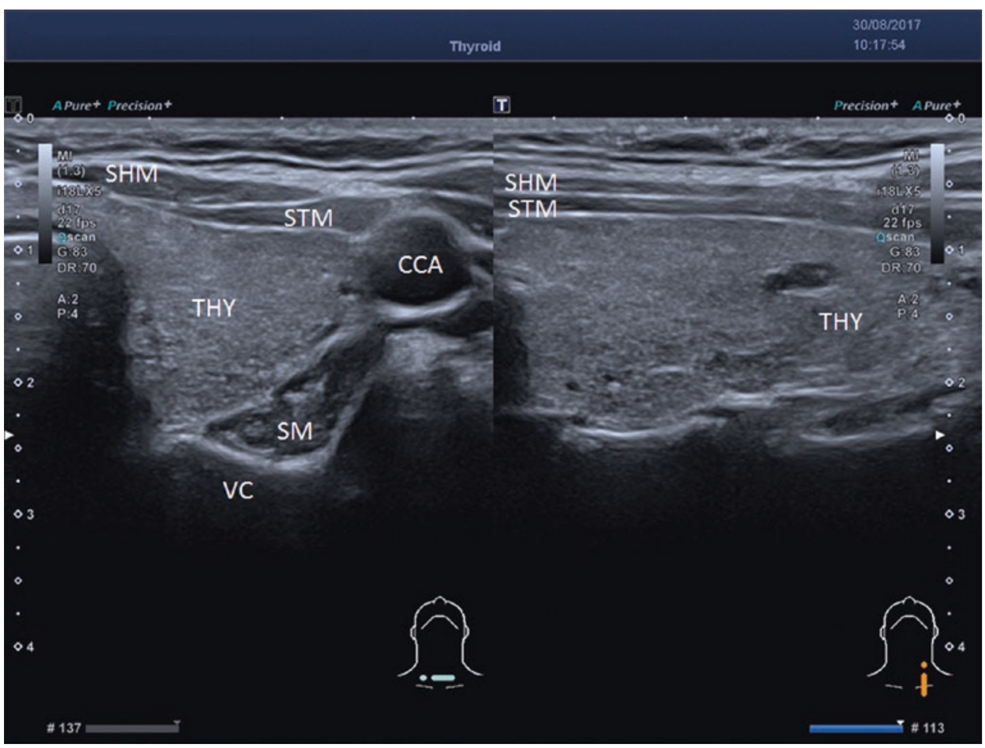

Fig. 3.4 Left thyroid lobe area, transverse plane (*left*) and sagittal plane (*right*). CCA common carotid artery, SHM sternohyoid muscle, SM scalene muscles, STM sternothyroid muscle, THY thyroid gland, VC vertebral column

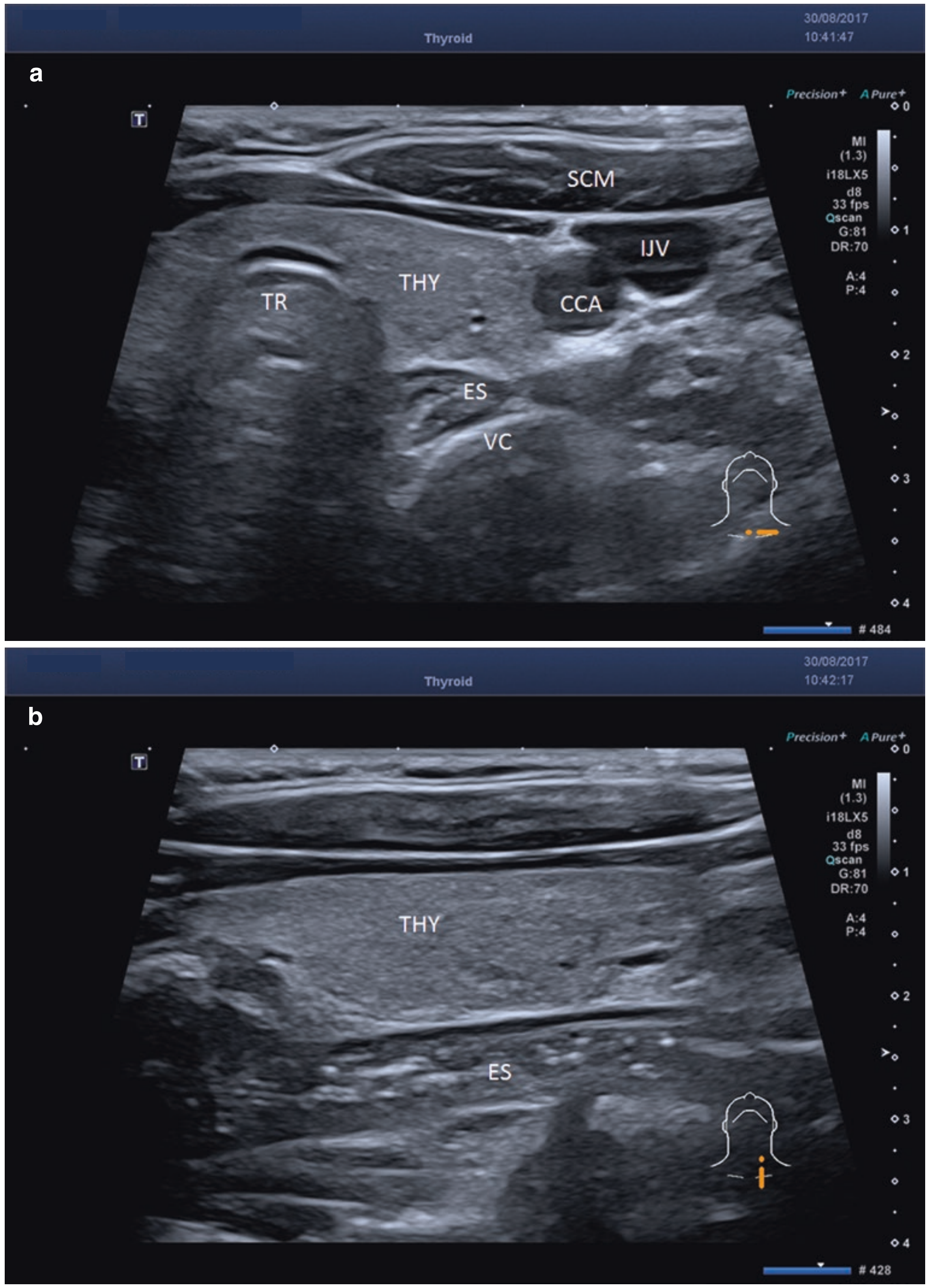

Fig. 3.5 Esophagus (ES) dorsal to the left thyroid lobe (THY), in transverse plane (**a**) and sagittal plane (**b**). CCA common carotid artery, IJV internal jugular vein, SCM sternocleidomastoid muscle, TR trachea, VC vertebral column

cases, the esophagus cannot be seen at all, because it can be completely covered by the acoustic shadow of the trachea.

The cricoid and thyroid cartilages can be seen cranial to the thyroid (Figs. 3.7 and 3.8). In younger patients, the cartilages are not ossified, which allows a sonographic view into the larynx. Then structures such as the vestibular folds can be examined (Video 3.4). With increasing ossification, the examination of intralaryngeal structures becomes more and more difficult, but not impossible [4].

3.3.2 The Jugular Fossa and the Supraclavicular Region

In clinical practice, it is often forgotten to examine the jugular fossa and the supraclavicular region, because most diseases of the head and neck become clinically apparent more cranially. Nevertheless, we have often found metastatic lymph nodes in this area, especially in patients suffering from thyroid cancer, breast cancer, or even colon or

Fig. 3.6 Esophagus (ES) next to the right thyroid lobe (THY). CCA common carotid artery, TR trachea

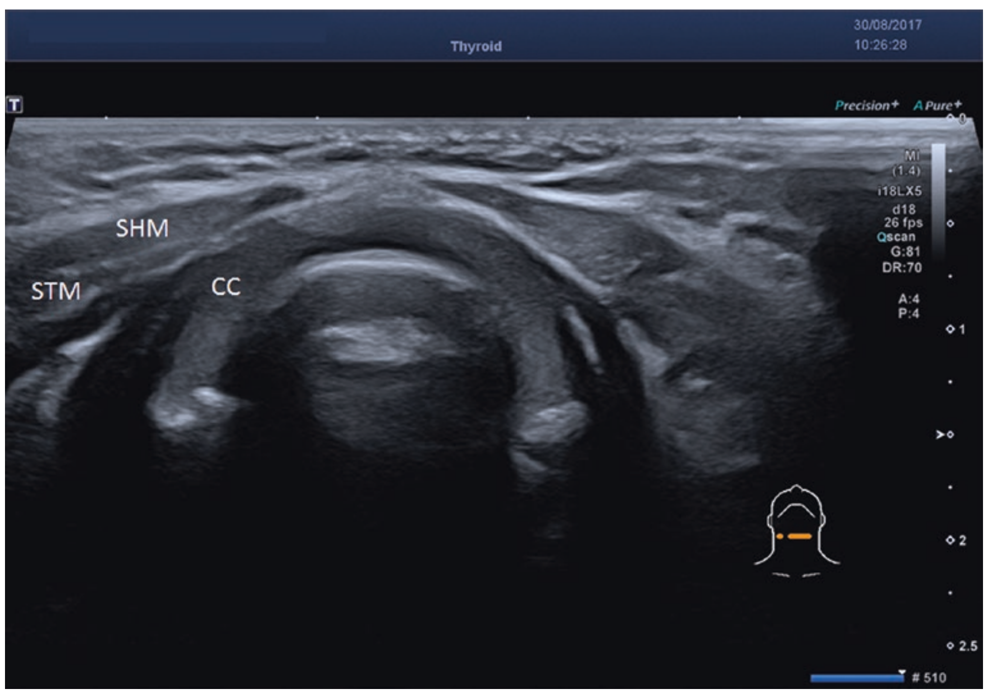

Fig. 3.7 Cricoid cartilage (CC). SHM sternohyoid muscle, STM sternothyroid muscle

prostate cancer. Furthermore, the sonographic examination of the jugular fossa allows a view into the upper mediastinum, where, for example, parathyroid adenomas can be found.

In young patients, parts of the thymus can be seen in the jugular fossa (Fig. 3.9). Likewise, in this area, blood vessels often can be seen in healthy patients. Thus, sometimes, the aortic arch becomes visible (Fig. 3.10). Furthermore, the brachiocephalic artery, the supraclavicular artery, and the common carotid artery can be detected next to the pleura (Figs. 3.11 and 3.12). At last, in this area, the nerves of the cervical plexus can be seen well between both scalene muscles (Figs. 3.13 and 3.14), allowing ultrasound-guided plexus anesthesia.

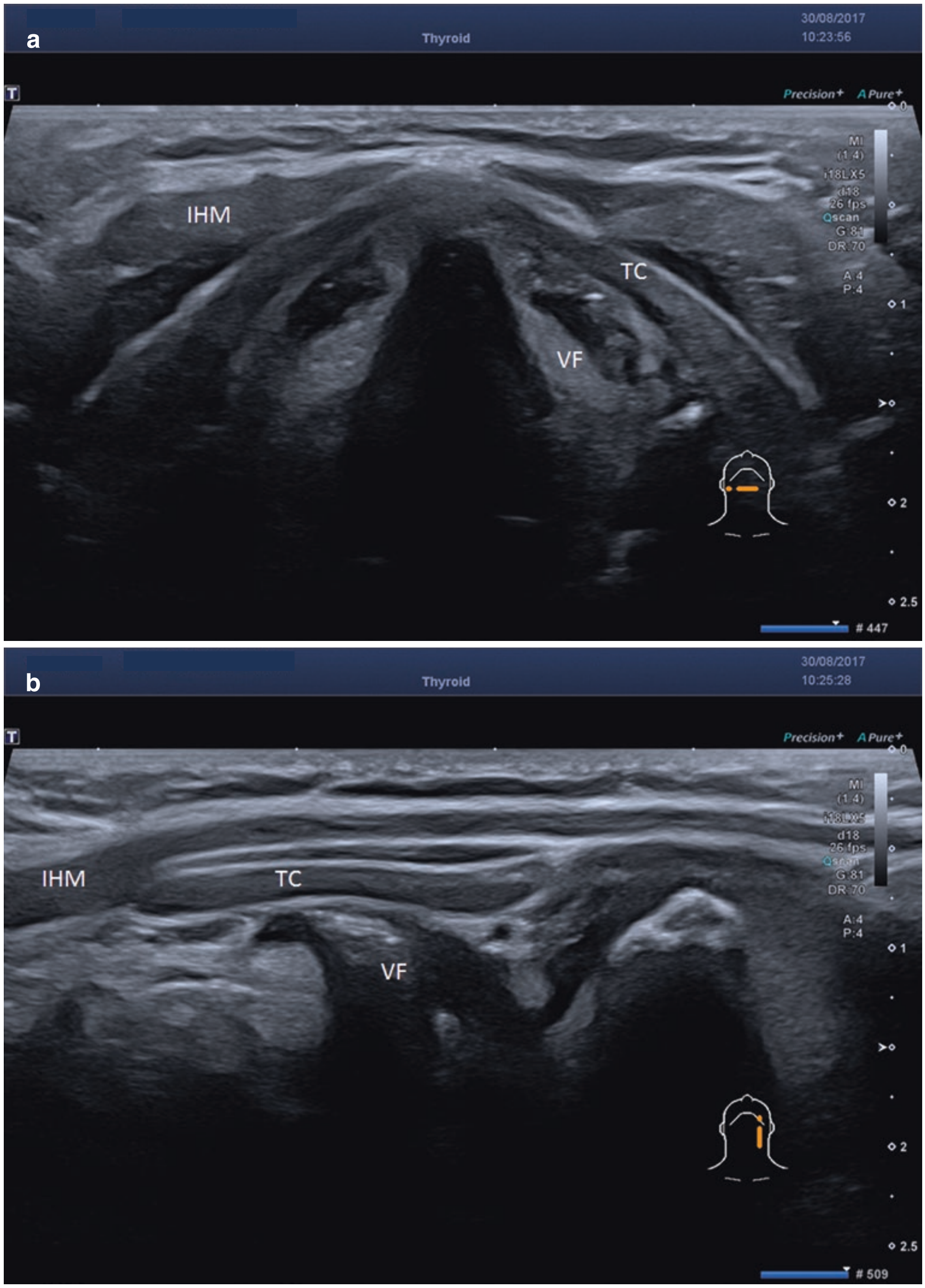

Fig. 3.8 Transverse (**a**) and sagittal (**b** and **c**) sections through the larynx at the level of the thyroid cartilage (TC). IHM infrahyoid muscle, SHM sternohyoid muscle, STM sternothyroid muscle, THM thyrohyoid muscle, VF vestibular fold

Fig. 3.8 (continued)

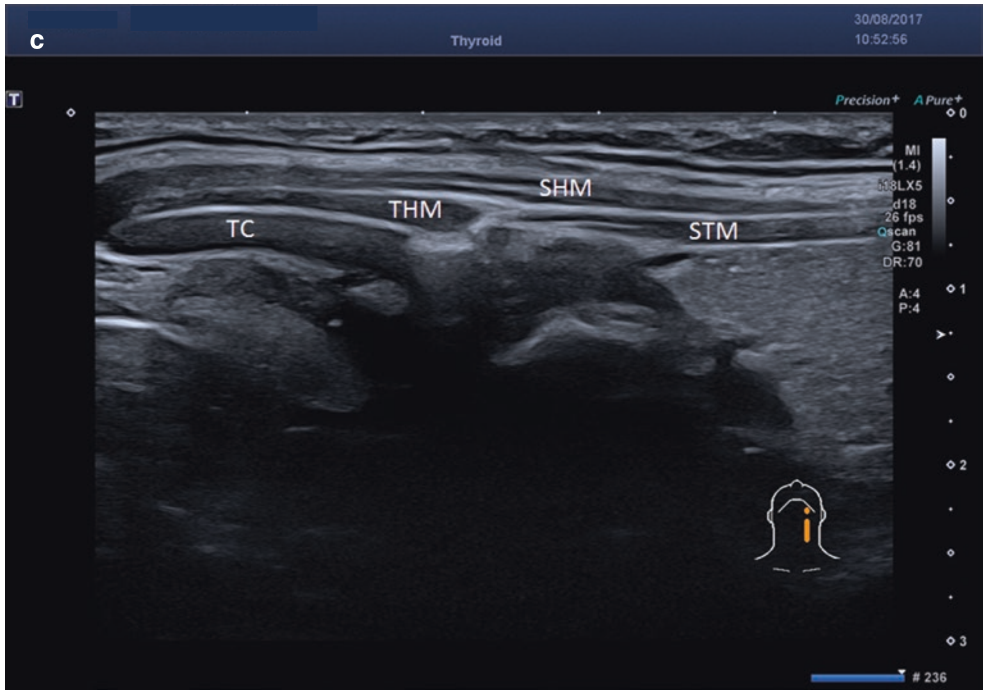

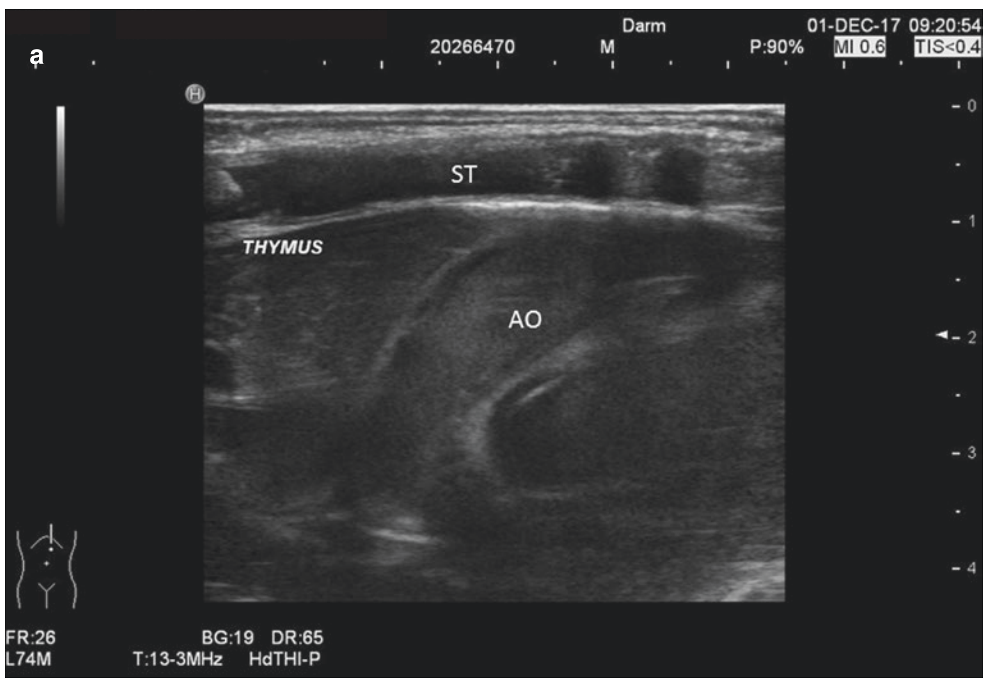

Fig. 3.9 In children, the thymus can be detected in the upper mediastinum through the sternum (**a**) and sometimes also through the jugular fossa (**b**). AO aorta, CL clavicle

Fig. 3.9 (continued)

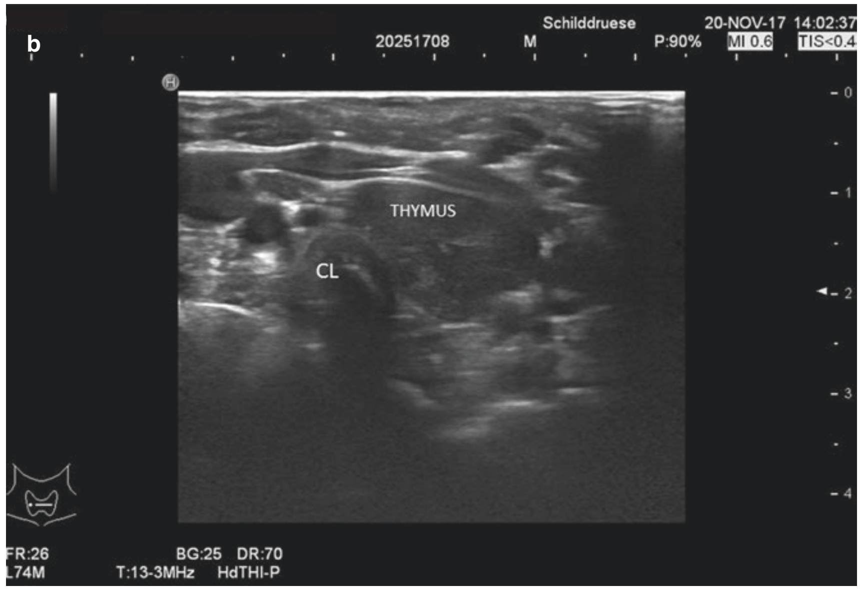

Fig. 3.10 The jugular fossa with the arch of the aorta (AO). (**a**) B-Scan and color-coded sonography. (**b**) Doppler sonography

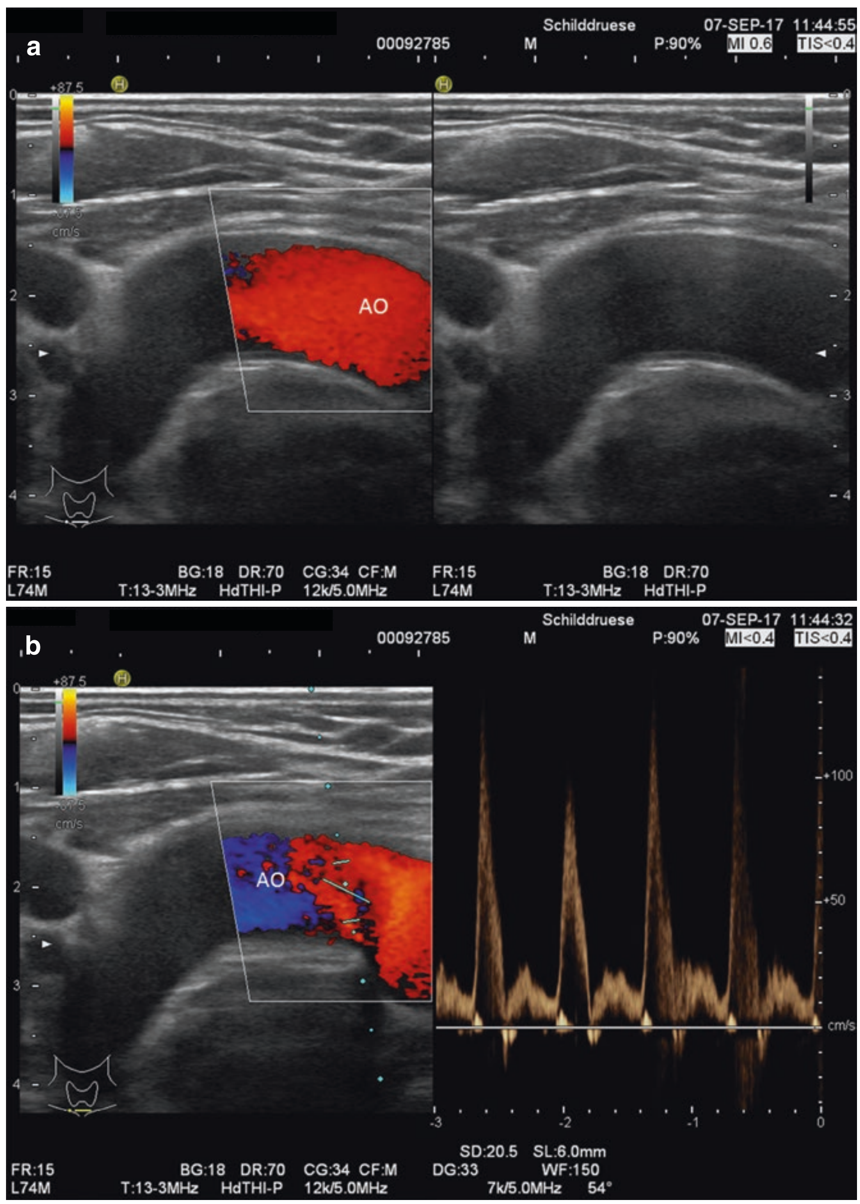

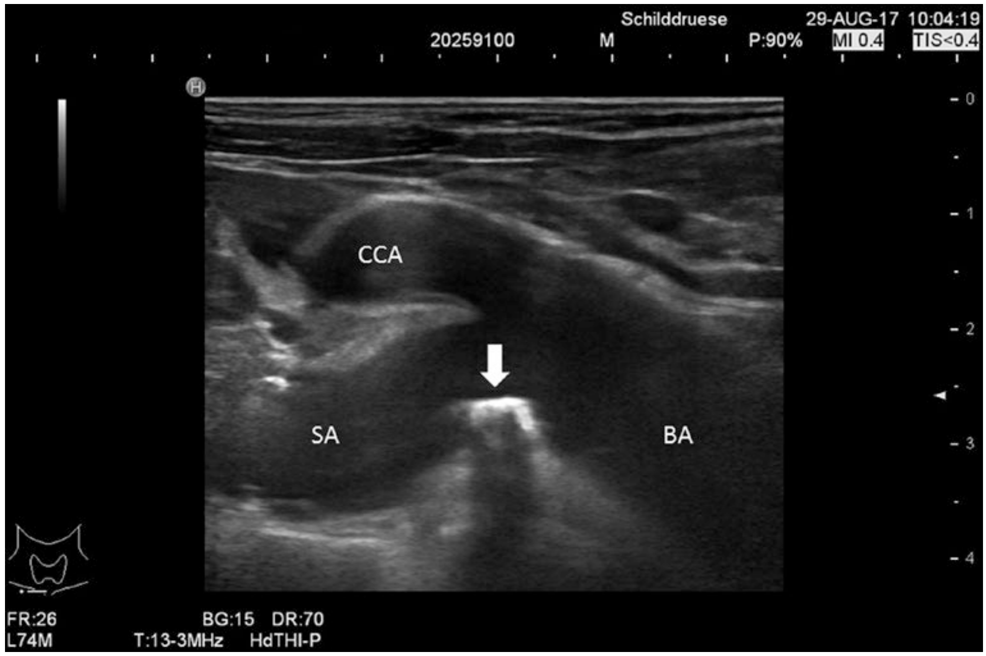

Fig. 3.11 Right supraclavicular region with the brachiocephalic artery (BA) and its bifurcation; the *arrow* indicates a calcified plaque. CCA common carotid artery, SA supraclavicular artery

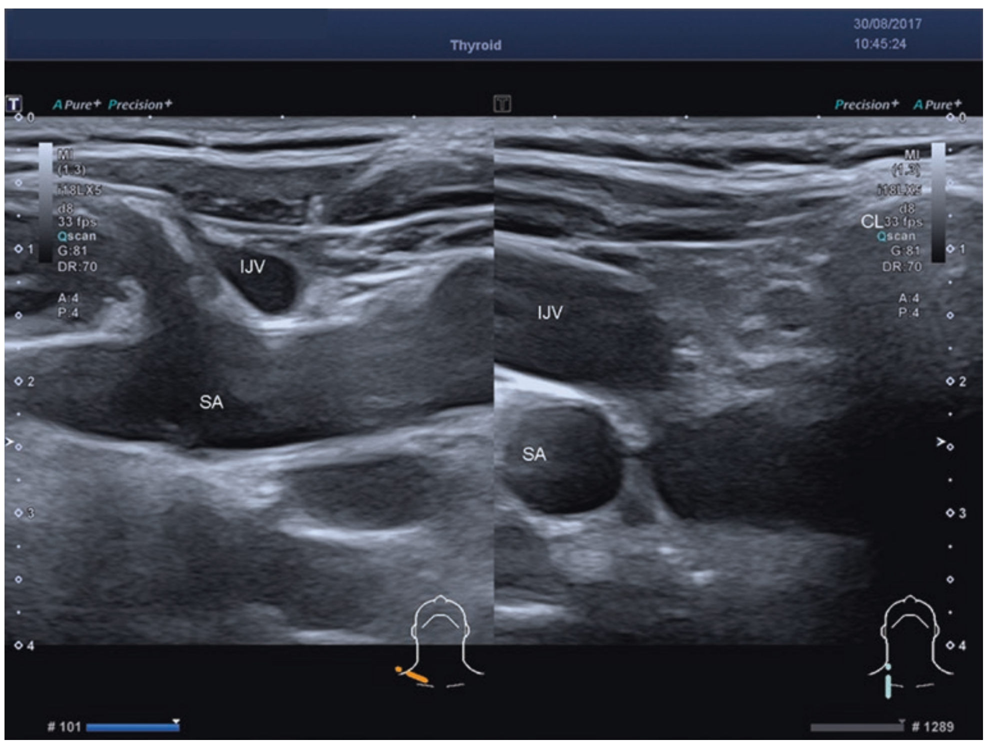

Fig. 3.12 Right supraclavicular region, transverse plane (*left*) and sagittal plane (*right*). CL clavicle, IJV internal jugular vein, SA supraclavicular artery

3.3.3 The Lateral Neck Compartment

The examination of the lateral neck compartments starts with the general view through the appropriate thyroid lobe, the large blood vessels, and the sternocleidomastoid muscle (Fig. 3.15). Too much pressure with the array on the patient's neck results in a collapse of the internal jugular vein. In contrast to the common carotid artery, the wall of the vein is very thin, and sometimes venous valves can be detected (Fig. 3.16; (Video 3.5). The external jugular vein can be seen in the superficial area of the lateral neck (Fig. 3.17). The omohyoid muscle (Fig. 3.18) is characterized by an oblique course in this area. This muscle is located between the sternocleidomastoid muscle and the large vessels and can easily be misdiagnosed as a lymph node in this area.

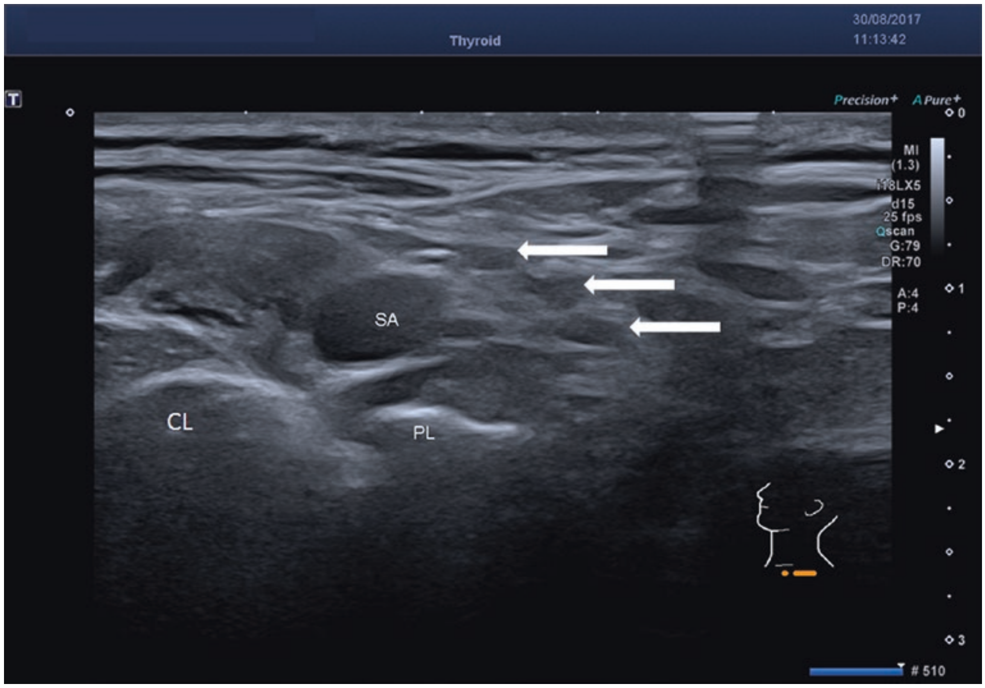

Fig. 3.13 Left supraclavicular region with parts of the supraclavicular plexus (*arrows*). CL clavicle, PL pleura, SA supraclavicular artery

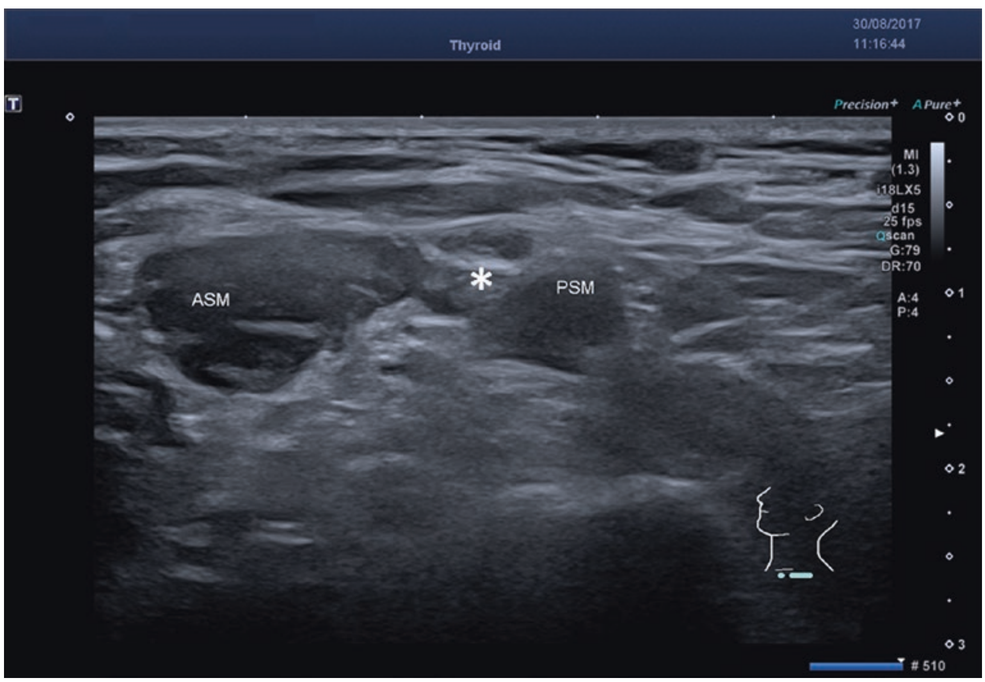

Fig. 3.14 Parts of the cervical plexus (*asterisk*) can be seen between the anterior scalene muscle (ASM) and the posterior scalene muscle (PSM)